Polarization-dependent losses in porous silicon ridge waveguides

F. Cassio, L. Poffo, N. Lorrain, P. Pirasteh, J. Lemaitre, M. Guendouz

Results in Optics 9 (2022) 100269

Contents lists available at ScienceDirect

Results in Optics

journal homepage: www.sciencedirect.com/journal/results-in-optics

Polarization-dependent losses in porous silicon ridge waveguides

F. Cassio, L. Poffo *, N. Lorrain, P. Pirasteh, J. Lemaitre, M. Guendouz

UMR FOTON, CNRS, Université de Rennes 1, Enssat, F22305 Lannion, France

ARTICLE INFO

Keywords:
Porous silicon ridge waveguide
Integrated optics
Optical sensor
Polarization light

ABSTRACT

Porous silicon is a material used in integrated optics with few studies on its structuration impact on the polarization in the near infra-red spectral range. In this letter, we report experimental results from optical characterizations around the wavelength of 1550 nm and for different input polarization in porous silicon ridge waveguides. We highlight filtering of light polarization that attenuates transverse electric mode in passive porous silicon ridge waveguides.

1. Introduction

Porous silicon (PSi) is a structured material produced by electrochemical anodization of a silicon substrate in a diluted hydrofluoric acid electrolyte (Zhang et al., 1989). The manufacturing process allows to control the porosity (and then the refractive index), the pore size and the thickness of the porous layers. Then it makes possible to manufacture several optical devices composed of one or more successive layers such as for example waveguides, Bragg mirrors and microcavities (Jane et al., 2009; Arshavsky-Graham et al., 2018; De Stefano, 2019). The pore morphology depends on the type and the level of doping as well as the crystalline orientation of the silicon substrate. A columnar mesoporous morphology is obtained with a heavily doped P silicon substrate with a (1 0 0)-orientation (Zhang, 2005). This kind of structured material normally depends on the polarization. In this paper, we present the effect of input signal polarization on light propagation in passive PSi single mode ridge waveguides.

Few studies deal with the impact of the PSi structuration on the polarization of light. Lower optical losses for transverse magnetic (TM) modes than those for transverse electric (TE) modes were measured in PSi multimode planar waveguides that could be related to PSi anisotropic morphology (Charrier et al., 2012). Moreover, in an asymmetric active waveguide composed of a Bragg mirror cladding with a luminescent core on the top, TE polarization luminescence modes are guided whereas the TM modes are absorbed (Escobar et al., 2018). A correlation between the polarization of visible photoluminescence and the degree of polarization has been determined in PSi structures excited by polarized light, but regardless of their morphology (Andrianov et al., 1993; Koyama and Koshida, 1995).

In integrated optics applications, a polarization control device is used to increase optical performances like a contrast in a microresonator, but the real impact of the polarization light input in single-mode ridge waveguides has not been studied yet.

In this letter, we present the effect of the polarization input signal in single-mode PSi ridge waveguides by studying the filtering attenuation of the transmission light. The optical characterizations were carried out around the wavelength of 1550 nm by controlling the type of the polarization.

2. Methods

Studied PSi ridge waveguides were fabricated by a standard photolithographic process from four consecutive PSi layers prepared by electrochemical anodization of a heavily doped P (1 0 0) silicon substrate with a resistivity of 5 mΩ.cm at a room temperature maintained at 18 °C (Cassio et al., 2020).

In this study, four layers were needed to elaborate the waveguide. Indeed, in addition to the guiding and the cladding, two thin barrier layers with low porosity which sandwiching the guiding layer were necessaries to prevent resin infiltration inside of the guiding and the cladding layers during the photolithographic process used fabricate the PSi ridge waveguide.

The waveguide dimensions have to be chosen to provide single mode propagation at 1550 nm. In order to define the width and height of the ridge PSi waveguide constituted of a core layer and a cladding layer with a refractive index of 1.57 and 1.41 respectively (Fig. 1.a). The lowest dimension limits (width and height) of the 00, 01 and 10 TE and TM modes propagation that involve solutions to the Maxwell equations have

* Corresponding author.
E-mail address: luiz.poffo@univ-rennes1.fr (L. Poffo).

https://doi.org/10.1016/j.rio.2022.100269
Received 10 May 2022; Received in revised form 1 July 2022; Accepted 11 July 2022
Available online 16 July 2022

been calculated and reported in Fig. 1.b and Fig. 1.c. The blue area between the lowest limits of the 00 mode (fundamental mode), the 01 and 10 modes, represents the single mode propagation region. For TM modes, the curves are similar to TE modes but are slightly shifted towards higher dimension values. Thus, the results indicate the range of width and height of PSi ridge waveguide that allow single mode propagation. Based on these theoretical results, a width of 2 μm and a height of 1.5 μm were aimed at obtaining a single-mode propagation for both TE and TM polarization.

Then, other simulations, performed with a Film Mode Matching solver commercialized by Photon Design, were performed and showed that the thickness of the barrier layers must not exceed 40 nm to allow a single mode propagation in the core layer. According to the simulations, a thickness of 30 nm was chosen for the barrier porous layers.

The four layers with well-defined thicknesses were prepared by successively applying four current densities for specific times. The current densities for each layer of the PSi ridge waveguide were chosen to obtain refractive indices of 2.27, 1.57, 2.27 and 1.41 respectively (Cassio et al., 2020). The Fig. 2a shows the cross-section of the obtained layers with columnar pores. The thicknesses were measured by microscopy (SEM) and are respectively of 30 nm, 1.6 μm, 30 nm and 4.7 μm.

The cross section of the etched ridge waveguide is reported in Fig. 2.b showing the PSi guiding with almost the aimed dimensions (width of 1.95 μm and a height of 1.6 μm). Before the optical characterizations of the fabricated PSi ridge waveguide, some preliminary simulations have been carried out taking into consideration the experimental waveguide dimensions obtained by SEM observations.

Optical characterizations were investigated using the optical bench described in Fig. 3. The input optical signal from a fibered broadband tunable laser source set at 1550 nm (Yenista Tunics T100S-HP) is injected into the PSi ridge waveguide using a micro-lensed polarization-maintaining fiber with a mode radius of 2 μm. The coupling losses have been estimated at 7 dB (Thual et al., 2005).

The input polarization is set with a fiber rotator mounted on the micro-alignment bench which permit to inject in the PSi ridge waveguide either the TE mode, the TM mode or an equal distribution of both polarizations. The polarization modification induced by the micro-lens is considered negligible (Thual et al., 2005) and it was verified by a polarimeter to ensure accurately the polarization input laser. The output signal is collected with a second micro-lensed fiber and sent to a power meter.

Between each measurement of output power, the length of the waveguides is reduced by cleaving and the sample slices are polished to optimize the coupling between the fibers and the waveguides.

3. Results

For the different input polarizations, we measured the output power for different lengths of the waveguides as shown in the Table 1. Each measurement is repeated three times to obtain the uncertainty on the value.

We plotted, in Fig. 4, the output power in function of the waveguide length for the three different input polarization configurations.

We can notice the presence of two distinct zones, noted A and B on the figure. By exploiting the tendency curves of the three configurations in zone A, we deduced propagation losses of the order of 18 dB/cm for the TM mode or for an equal distribution of TM and TE modes. However, for the TE mode, the power detected at the output corresponds to the noise of the detector, in other words, no signal was detected. The 3 dB attenuation between the ordinates at the origin of the first two configurations illustrates the complete extinction of the TE mode. In area B, below a length of 2.3 mm, specific to the experimental conditions, the TE mode is not totally attenuated.

The exploitation of the trend curves in zone B allowed us to estimate propagation losses of the order of 18 dB/cm, 34 dB/cm and 116 dB/cm, still for the three different input polarization configurations respectively.

4. Discussion

Under the manufacturing conditions we used for this study, porous silicon (PSi) waveguides present high propagation losses, around 18 dB/cm. These high losses are mainly due to the adsorption of the free carriers of the P type silicon substrate (Chan et al., 1996), more than the surface scattering losses induced by the surface roughness and the volume scattering depending on the pore diameters (Azuelos et al., 2018; Pirasteh et al., 2007). To reduce the losses, a thermal oxidation treatment of PSi layers could be performed. However, despite high losses, PSi is widely used in the field of label free biosensors (De Stefano, 2019; Azuelos et al., 2018), due to its large surface specific area and its biocompatibility. So, as the main application of PSi is biosensing, in order to reduce the losses in the whole optical biosensor, we planned to implement a hybrid structure by associating the PSi transducer MR with a polymer bulk waveguides which will ensure the transmission and recovery of the optical signal (Cassio et al., 2020).

Propagation losses had been estimated at 116 dB/cm for TE mode, showing a 6.5 times higher attenuation of the TE mode compared to the TM mode. So, the PSi material would act as a filter allowing only the TM component polarization to pass through and would totally attenuate the TE component polarization.

This filtering effect can be associated to the morphology of the PSi

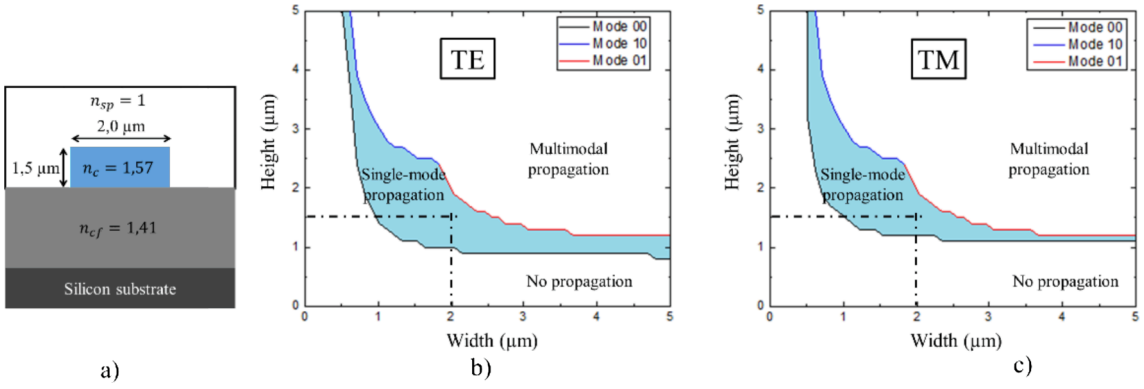

Fig. 1. Schematization of the PSi ridge waveguide with a core layer of width and height. The thin (around 30 nm) barrier layers are not represented (a). Determination of the single-mode propagation region at the working wavelength of 1.55 μm after numerical calculation of the effective index of a two-dimensional waveguide, for the polarization modes TE 00, 01 and 10 (b), and TM 00, 01 and 10 (c). The refractive indices of the superstrate nsp, core nc and cladding ncf are respectively 1, 1.57 and 1.41.

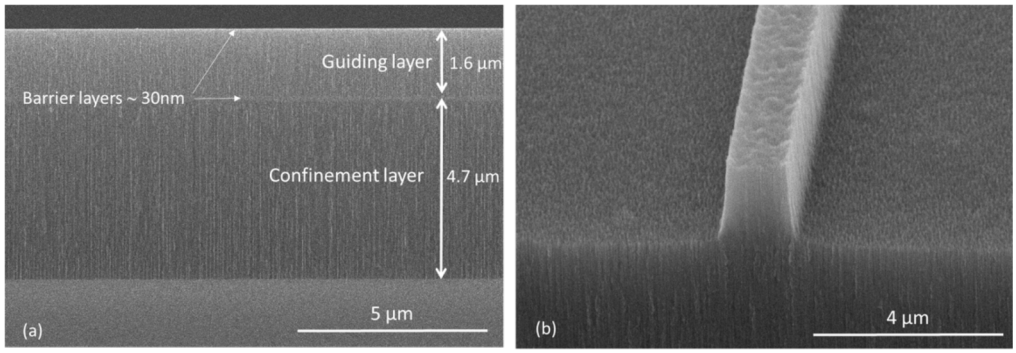

Fig. 2. SEM cross section observations of the PSi layers (a) before and (b) after photolithography process.

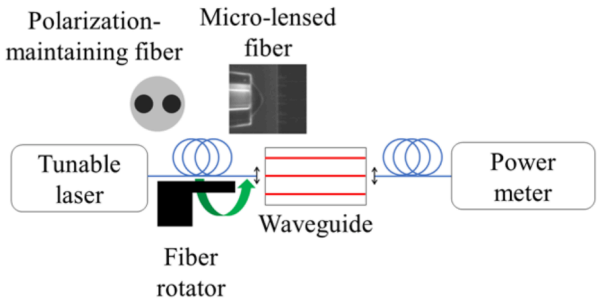

Fig. 3. Schematic representation optical bench for optical characterizations.

Table 1
Output power for different input polarizations as a function of the waveguide length.

Waveguide length (cm)	Output power (dBm) TM	Output power (dBm) 50 % TM/50 % TE	Output power (dBm) TE
0.60	−35.1 ± 0.5	−38.1 ± 0.8	−50.2 ± 1.6
0.51	−33.4 ± 0.9	−36.5 ± 0.5	−50.2 ± 1.3
0.41	−31.7 ± 0.6	−34.7 ± 0.6	−50.2 ± 1.3
0.31	−30.0 ± 0.5	−33.0 ± 0.9	−50.2 ± 1.4
0.22	−28.3 ± 0.8	−31.3 ± 0.6	−43.3 ± 1.1
0.19	−27.7 ± 0.6	−30.4 ± 0.7	−43.0 ± 1.1
0.16	−27.3 ± 0.8	−29.5 ± 0.8	−40.5 ± 1.2
0.13	−26.8 ± 0.8	−28.4 ± 0.9	−36.3 ± 0.9
0.11	−26.5 ± 0.9	−28.0 ± 0.8	−34.4 ± 0.9

layers obtained from heavily P doped Silicon substrate oriented (1 0 0): the vertical columnar pores structure would allow the TM component to pass through parallel to the pores. This hypothesis had also been put forward by Charrier et al. (2012) to explain the lower losses for TM modes that had been obtained in PSi multimode planar waveguides.

In addition, the heavily doped silicon is semi-metallic and could give rise to plasmonic resonances for the TE mode, which could also explain the observed phenomenon (Majorel et al., 2019).

5. Conclusion

In this letter, we presented the optical characterization and the polarization effect of PSi ridge waveguides. The PSi layers were made by electrochemical anodization from a heavily doped P-oriented (1 0 0) silicon substrate, giving a columnar mesoporous morphology of the pores. We have demonstrated a filtering of 116 dB/cm of the TE mode polarization which we attributed to the PSi morphology. This phenomenon could be of interest in integrated optics devices to reduce propagation losses due to poor polarization control. It would therefore

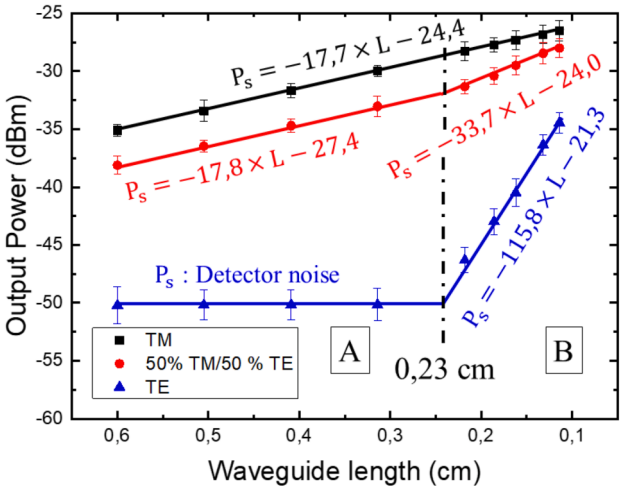

Fig. 4. Evolution of the output power for different waveguide lengths for the three configurations studied: TM, 50% TM/50% TE and TE.

be necessary to inject a polarization controlled optical signal into the guiding layer of PSi, in order to reduce the already high optical losses in this material that are inherent to its porous nature.

Declaration of Competing Interest

The authors declare that they have no known competing financial interests or personal relationships that could have appeared to influence the work reported in this paper.

Acknowledgements

Technical processing of porous silicon ridge waveguides were performed in the CCLO-Renatech clean room facilities of Foton institute. This work is funded by Lannion Trégor Community (LTC22) and Région de Bretagne.

References

Andrianov, A.V., Kovalev, D.I., Zinov'ev, N.N., Yaroshetskii, I.D., 1993. Anomalous photoluminescence polarization of porous silicon. JETP Lett. 58, 427–430.
Arshavsky-Graham, S., Massad-Ivanir, N., Segal, E., Weiss, S., 2018. Porous silicon-based photonic biosensors: current status and emerging applications. Anal. Chem. 91, 441–467. https://doi.org/10.1021/acs.analchem.8b05028.
Azuelos, P., Girault, P., Lorrain, N., Dumeige, Y., Bodiou, L., Poffo, L., Guendouz, M., Thual, M., Charrier, J., 2018. Optimization of porous silicon waveguide design for micro-ring resonator sensing applications. J. Opt. 20 (8), 085301–085314. https://doi.org/10.1088/2040-8986/aad01b.
Cassio, F., Lorrain, N., Pirasteh, P., Poffo, L., Lemaitre, J., Hardy, I., Guendouz, M., 2020. Porosity calibration in a 4-layer porous silicon structure to fabricate a micro-resonator with well-defined refractive indices and dedicated to biosensing

applications. Opt. Mater. 110, 110468 https://doi.org/10.1016/j.optmat.2020.110468.
Chan, M.H., So, S.K., Cheah, K.W., 1996. Optical absorption of free standing porous silicon films. J. Appl. Phys. 79 (6), 3273–3275. https://doi.org/10.1063/1.361216.
Charrier, J., Dumeige, Y., Pirasteh, P., Gadonna, M., 2012. Effect of interface roughness and polarization on the optical losses of porous silicon-based waveguides. Micro. Nano. Lett. 7, 275–278. https://doi.org/10.1049/mnl.2012.0027.
De Stefano, L., 2019. Porous silicon optical biosensors: still a promise or a failure? Sensors 19, 4476. https://doi.org/10.3390/s19214776.
De Stefano, L., 2019. Porous silicon optical biosensors: still a promise or a failure? Sensors 19, 4776–4784. https://doi.org/10.3390/s19214776.
Escobar, S., Nava, R., Flores-Romero, E., Reyes-Esqueda, J.A., 2018. Light polarization in active photonic waveguides of porous silicon. Photonic. Nanostruct. 31, 44–51. https://doi.org/10.1016/j.photonics.2018.05.009.
Jane, A., Dronov, R., Hodges, A., Voelcker, N.H., 2009. Porous silicon biosensors on the advance. Trends Biotechnol. 27, 230–239. https://doi.org/10.1016/j.tibtech.2008.12.004.
Koyama, H., Koshida, N., 1995. Polarization retention in the visible photoluminescence of porous silicon. Phys. Rev. B 52, 2649–2655. https://doi.org/10.1103/PhysRevB.52.2649.
Majorel, C., Paillard, V., Patoux, A., Wiecha, P.R., Cuche, A., Arbouet, A., Bonafos, C., Girard, C., 2019. Theory of plasmonic properties of hyper-doped silicon nanostructures. Opt. Commun. 453, 124336 https://doi.org/10.1016/j.optcom.2019.124336.
Pirasteh, P., Charrier, J., Dumeige, Y., Haesaert, S., Joubert, P., 2007. Optical loss study of porous silicon and oxidized porous silicon planar waveguides. J. Appl. Phys. 101, 083110–083116. https://doi.org/10.1063/1.2718886.
Thual, M., Moreau, G., Ribette, J., Rochard, P., Gadonna, M., Simon, J.C., 2005. Micro-lens on polarization maintaining fibre for coupling with 1.55 μm quantum dot devices. Opt. Commun. 255, 278. https://doi.org/10.1016/j.optcom.2005.06.040.
Zhang, G.X., 2005. Porous silicon: morphology and formation mechanisms. Mod. Aspect. Electroc. 39, 65–133. https://doi.org/10.1007/978-0-387-31701-4_2.
Zhang, X.G., Collins, S.D., Smith, R.L., 1989. Porous Silicon Formation and Electropolishing of Silicon by Anodic Polarization in HF Solution. J. Electrochem. Soc. 136, 1561–1565. https://doi.org/10.1149/1.2096961.